© 2020. Published by The Company of Biologists Ltd | Journal of Experimental Biology (2020) 223, jeb214965. doi:10.1242/jeb.214965

RESEARCH ARTICLE

Humming hummingbirds, insect flight tones and a model of animal flight sound

Christopher J. Clark‡ and Emily A. Mistick*

ABSTRACT

Why do hummingbirds hum and insects whine when their wings flap in flight? Gutin proposed that a spinning propeller produces tonal sound because the location of the center of aerodynamic pressure on each blade oscillates relative to an external receiver. Animal wings also move, and in addition, aerodynamic force produced by animal wings fluctuates in magnitude and direction over the course of the wingbeat. Here, we modeled animal wing tone as the equal, opposite reaction to aerodynamic forces on the wing, using Lowson's equation for the sound field produced by a moving point force. Two assumptions of Lowson's equation were met: animal flight is low (<0.3) Mach and animals from albatrosses to mosquitoes are acoustically compact, meaning they have a small spatial extent relative to the wavelength of their wingbeat frequency. This model predicted the acoustic waveform of a hovering Costa's hummingbird (*Calypte costae*), which varies in the *x*, *y* and *z* directions around the animal. We modeled the wing forces of a hovering animal as a sinusoid with an amplitude equal to body weight. This model predicted wing sound pressure levels below a hovering hummingbird and mosquito to within 2 dB; and that far-field mosquito wing tone attenuates to 20 dB within about 0.2 m of the animal, while hummingbird humming attenuates to 20 dB at about 10 m. Wing tone plays a role in communication of certain insects, such as mosquitoes, and influences predator–prey interactions, because it potentially reveals the predator's presence to its intended prey.

KEY WORDS: Adventitious sound, Locomotion-induced sound, Gutin sound, Helmholtz number, Sonation, Trochilidae

INTRODUCTION

The whine of a mosquito right by one's ear may be among the most universal of human experiences. Flight tones of certain midge and mosquito species serve a communication role in courtship (Cator et al., 2009; de Silva et al., 2015). Other small animals make wing tones in flight, such as the buzzing of bees and flies, or the humming of hummingbirds and hawkmoths as they fly from flower to flower, for which a clear function has not been identified. Flight tones seem to be a ubiquitous feature of flapping wings. Most prior work on insect and hummingbird flight tones has centered on the observation that the dominant (highest amplitude) frequency of the flight tone is either the wingbeat frequency (Arthur et al., 2014; Sotavalta, 1952; Sueur et al., 2005; Webb et al., 1976; Williams and Galambos, 1950) or, from certain angles, double the wingbeat frequency (Bae and Moon, 2008; Dudley, 2000). Here, we explored the question: why does a flapping wing produce tonal sound that varies with orientation around the animal?

Acoustic theory developed for propellers suggests multiple possible mechanisms (Inada et al., 2009; Seo et al., 2019). A spinning rotor produces three types of sources of sound: monopole-like 'unsteady source of mass' (Bodony et al., 2016), where sound is produced by a volumetric process; dipole-like 'load' or Gutin sound (Fig. 1A), where sound is produced by a force; and quadrupole-like 'broadband' sound (Blake, 2017a; Howe, 2008; Magliozzi et al., 1981; Schmitz, 1981).

This third broadband noise term, on a wing, is primarily caused by ingestion, formation and scattering of turbulence and vorticity (at the leading edge, surface and trailing edge, respectively) (Blake, 2017b). Such sounds are widespread in animal flight, even in the relatively quiet flight of owls (Sarradj et al., 2011). But as this sound source type is broadband (atonal), it is not consistent with wing tone that is the subject of this paper, and cannot be its source.

Regarding the first monopole-like term, in a propeller spinning at a constant angular velocity, one type of volumetric process that generates sound is thickness noise, caused by the sudden (unsteady) volumetric displacement of air by the propeller as it passes through a control volume, where the air is displaced in proportion to the propeller's thickness. The effect of thickness noise is reduced at lower Mach numbers (Blake, 2017a; Glegg and Devenport, 2017). As animal flight is low Mach (see below), whether thickness noise could be a significant source of animal wing sounds is unclear. Other monopole-like sources encompassed by an 'unsteady source of mass' that are not present in a propeller spinning at constant velocity might nevertheless be present in animal flight (Bodony et al., 2016). For instance, in ordinary hovering, a bulk of air $Q(t)$ is moved from above the animal to below the animal with each flap of the wings (Fig. 1A). If this induced bulk flow were continuous (as it is across a propeller spinning at a constant rate), it would not produce sound (Lighthill, 1962). But because animal wings reciprocate, rather than rotate at a constant rate like a propeller, the movement of the bulk of air is unsteady rather than continuous, and Q fluctuates in pulses associated with each wingbeat (Fig. 1A). As the time derivative (dQ/dt) is not zero, this mechanism hypothetically might contribute to the sound produced by animal wings (Bodony et al., 2016).

Of the three source types, propeller theory suggests a likely source of wing tone is the second type of sound, the reaction to fluctuating aerodynamic force (Glegg and Devenport, 2017). Gutin (1948) was the first to identify lift and drag as a major source of tonal sound on rotating propellers. The blades of a propeller, if spinning at a constant rate in uniform air, each develop force, $F(i,t)$, that is invariant in a local frame of reference. The equal, opposite reaction to this aerodynamic force imparted on the wing is aerodynamic pressure, $P(i,t)$, exerted on the surrounding air

Department of Evolution, Ecology, and Organismal Biology, University of California, Riverside, Riverside, CA 92521, USA.
*Present address: Institute for Resources, Environment, and Sustainability, University of British Columbia, Vancouver, BC, Canada, V6T 1Z4.

‡Author for correspondence (cclark@ucr.edu)

C.J.C., 0000-0001-7943-9291

Received 18 September 2019; Accepted 18 August 2020

Journal of Experimental Biology (2020) 223, jeb214965. doi:10.1242/jeb.214965

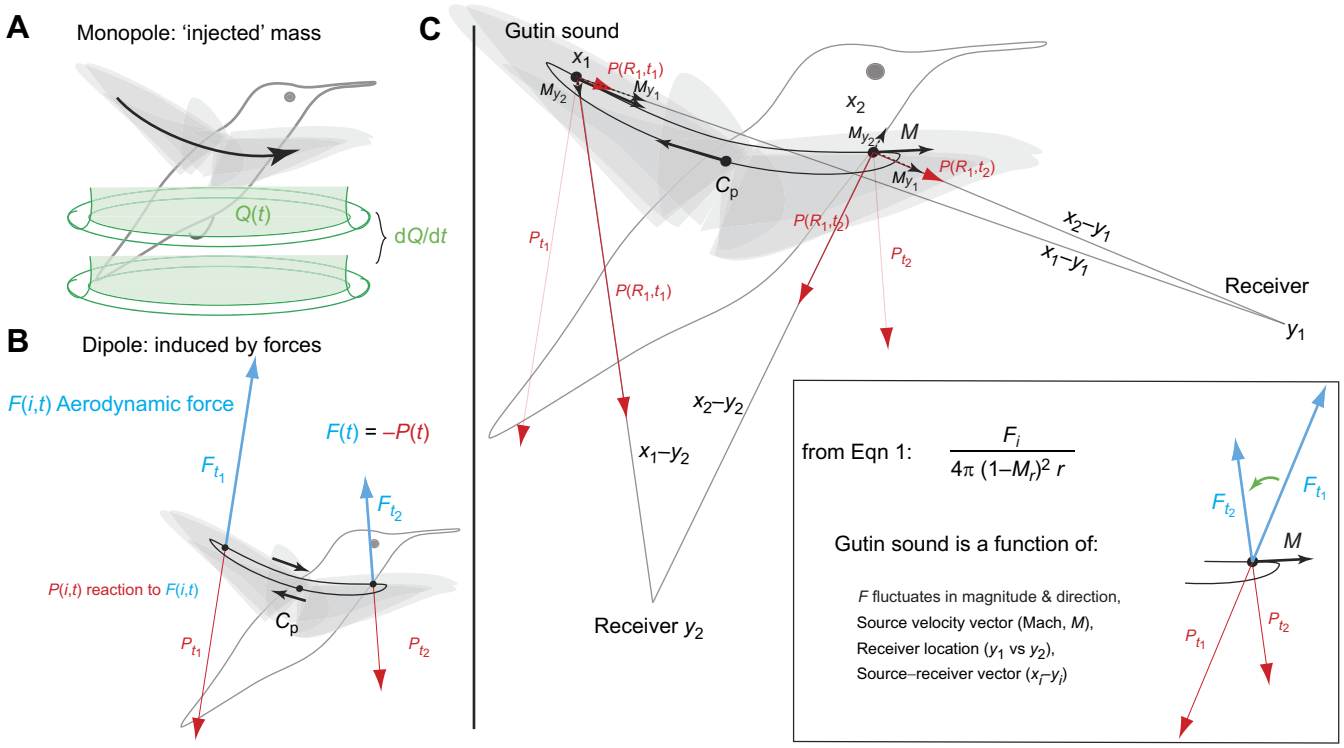

Fig. 1. Two hypothesized contributors to wing hum. (A) Monopole-like 'unsteady source of mass', such as the time derivative of bulk airflow ($\delta Q/\delta t$) induced by the wings, and (B,C) dipole-like Gutin sound arising from the reaction to production of aerodynamic forces. Sound arises from sources that are monopole, dipole or quadrupole (not shown) (Lighthill, 1962). (A) A hovering animal induces with its wings downwardly directed pulses of air (green); the time derivative of the induced flow, $\delta Q/\delta t$ could be a source of monopole-like sound. Another possible source is thickness noise (not shown; see Introduction). (B) Dipole sources are induced by forces (Lighthill, 1962). A flying animal produces aerodynamic force $F(i,t)$ with its wings (blue vectors). The pressure reaction $P(i,t)$ (red vectors) is the equal, opposite reaction to this aerodynamic force, a manifestation of Newton's 3rd law. Curved dark line: movement of the center of pressure, C_p. Note: vectors and trajectory of C_p are for illustration, not derived from data. (C) The Gutin sound pressure experienced in receiver locations y_1 and y_2 at two points in time. Symbols as in Eqn 1. The source x_i is modeled as a point source at the center of pressure, C_p, which moves through point x_1 at time t_1 and point x_2 at time t_2. Solid vectors are the pressure, $P(t)$ (red) and the velocity vector in Mach (M, black), of the source. Dashed vectors are the projection of the solid vector in the direction of the receiver (vector x_i–y_i) (grey lines). Inset: part of the nearfield term in Eqn 1 (Lowson, 1965). Curved line is trajectory of center of pressure. Receiver y_1 is approximately in-plane with the motion of the wings, while receiver y_2 is approximately orthogonal to the wing motion. Thus, receiver y_1 is primarily exposed to fluctuations in pressure that result from changes in drag, as modified by M_{y1} (the motion of the source relative to receiver y_1). Receiver y_2 is nearly orthogonal to the motion of C_p, and hence is primarily exposed to pressure changes caused by fluctuating lift, and the magnitude of M_{y2} is lower than that of M_{y1}.

(Fig. 1B), a manifestation of Newton's 3rd law (Blake, 2017a). As the force is invariant, so is the pressure. An observer spinning in the frame of reference of the propeller would not experience any fluctuation in pressure, and hence hears nothing. But Gutin (1948) reasoned that, as the location of the center of pressure on each blade oscillates relative to an external receiver, this external receiver experiences fluctuating pressure associated with the source's oscillatory motion. Because thrust is perpendicular to the plane of the spinning propeller, while drag is parallel to this plane, a receiver in front or behind the plane of the propeller hears sound generated in reaction to the rotating sources of thrust (except exactly on the central axis of the propeller, where the distance between the center of pressure and the receiver does not fluctuate, and thus there is no sound). A receiver to the side (in plane with the propeller) instead hears sound that is the aerodynamic reaction to drag (Blake, 2017a). This Gutin sound has a property of wing tone: it is tonal and varies with orientation around a propeller.

The wings of flying animals are similar to propellers: the wing moves (black solid vectors in Fig. 1C). Additionally, unlike the idealized propeller just described, the aerodynamic force vector on flapping wings (Fig. 1B, blue vectors) itself also varies substantially in magnitude and direction over the course of the wingbeat (Sane and Dickinson, 2001). The time derivative of force, $\delta F(i)/\delta t$ and the corresponding pressure, $\delta P(i)/\delta t$, are not zero. Thus, a flapping animal wing may produce sound during flight, caused by fluctuations in magnitude, direction and location of $F(i,t)$ on the wing, which generate fluctuations in pressure that a stationary receiver perceives as sound (Fig. 1C).

Here, we modeled this Gutin sound produced by the wings of a hovering hummingbird, using Lowson's (1965) equation for the sound field produced by a moving point force. Recent models of insect wing sound (Inada et al., 2009; Nedunchezian et al., 2019; Seo et al., 2019) have instead used the Ffowcs Williams–Hawkings (FW–H) equation (Ffowcs Williams and Hawkings, 1969). The FW–H equation was a refinement of Lowson's equation, as Lowson's equation becomes singular as speed approaches Mach (M)=1, while the FW–H equation does not suffer from this limitation. The FW–H equation provides the sound field produced by a moving surface pressure distribution, rather than Lowson's moving point force. While the FW–H equation is accurate as speed approaches M=1, using it requires the time history of the pressure distribution on a source, for instance, as computed with a computational fluid dynamics (CFD) model of the aerodynamic forces on an animal's wing (Seo et al., 2019). Lowson's equation instead requires an estimate of a point force (such as on the center of pressure of the wing).

Lowson's assumption of low Mach was not safe for propellers, but is safe for animal flight, where low Mach means $M<0.3$ (Glegg and Devenport, 2017). The Mach number is non-dimensional speed relative to the speed of sound (c), which for room-temperature air is roughly 340 m s^{-1}. The fastest flying extant animal is a falcon diving at 70 m s^{-1} (Tucker, 1998), which is a speed of Mach ∼0.2, while the wingtip of a hovering hummingbird reaches roughly ∼10 m s^{-1}, or Mach 0.03 (Clark and Mistick, 2018). Insect wingtips flap at even lower Mach numbers. Only one (extinct) biological structure has been suggested to have been supersonic: the whipped tip of a sauropod tail (Myhrvold and Currie, 1997). Aerodynamic models that are only valid at low Mach numbers are likely valid for nearly all biological applications.

Lowson's other important assumption was that his point force was acoustically compact, with a Helmholtz number of $\ll 1$. This Helmholtz number, also called the *ka* product, is a dimensionless number that describes sound source size relative to the wavelength of sound it produces (Larsen and Wahlberg, 2017). The parameter a is a characteristic source radius (treating the source as a sphere), such as animal wing length; and k is the wavenumber, $k=2\pi n/\lambda$, where λ is the wavelength associated with the wingbeat frequency (f) ($\lambda=c/f$) (Larsen and Wahlberg, 2017), and n is an integer harmonic of the wingbeat ($n=1$ is the fundamental, $n=2$ is the 2nd harmonic, etc.).

Here, we used wing hum of a hovering hummingbird as a test case for this model, as hummingbirds have wing hum that is salient to humans, and have been the subject of a CFD model of wing force in the three cardinal directions around the hovering animal (Song et al., 2014). Then, we generalized the model for the sound field directly below a hovering animal, by assuming that hovering animals produce aerodynamic force sinusoidally with an amplitude equal to body weight. We assessed this model against literature values for bird and insect wing sounds. Finally, we discuss the biological implications (communication and predator–prey interactions) of this sound field generated by a flapping wing.

MATERIALS AND METHODS

The model

The equation for pressure from a moving point force is (modified from Bodony et al., 2016; Lighthill, 1962; Lowson, 1965):

$$P(i,t)=\frac{\rho}{4\pi r(1-M_r)}\frac{\delta Q}{\delta t}+\frac{F_i}{4\pi(1-M_r)^2r^2}\left(\frac{(x_i-y_i)(1-M^2)}{r(1-M_r)}-M_i\right)+\frac{x_i-y_i}{4\pi cr^2(1-M_r)^2}\left(\frac{\delta F_i}{\delta t}+\frac{F_i}{1-M_r}\frac{\delta M_r}{\delta t}\right), \quad (1)$$

where $P(i,t)$ is the pressure over time in the i direction; $\delta Q/\delta t$ is the unsteady source of mass; ρ is air density; c is the speed of sound, roughly 340 m s^{-1} in air; F_i is the wing force vector in the i direction; M is the Mach number of the wing's motion; t is time; r is the scalar distance between source and receiver; and x and y are the locations of the receiver and source, respectively, such that $x_i–y_i$ is the vector distance between source and receiver. The subscript i indicates 'in the i direction', i.e. the term is the dot product between the vector ($x_i–y_i$) and the vector subscripted (M or F). Note that we have ignored the 'retarded time' (the propagation delay from source to receiver caused by finite speed of sound, c), as we will apply this equation to hovering animals (Fig. 1C).

The left-hand term containing $\delta Q/\delta t$ of Eqn 1 is the unsteady source of mass term described previously. The central and right terms are the Gutin sound. The central term containing F_i is the nearfield generated by the aerodynamic force (eqn 18 in Lowson, 1965), which scales as r^{-2}, as ($x_i–y_i$) is proportional to r. The right-hand term containing $\delta F_i/\delta t$ is farfield pressure, which scales as r^{-1}.

By taking the Doppler factor M_r to approximate to zero, many of the terms in Eqn 1 simplify to zero. If we also set $\delta Q/\delta t=0$, and neglect the farfield term, the predicted sound nearfield is:

$$P(i,t)=\frac{F(i,t)}{4\pi r^2}. \quad (2)$$

That is, in the nearfield, the magnitude of sound in the i direction is proportional to the aerodynamic force (F_i) on the wings oriented in the i direction, and inversely proportional to distance squared. In turn, considering only the farfield yields:

$$P(i,t)=\frac{\delta F(i)/\delta t}{4\pi cr}. \quad (3)$$

In the farfield, the magnitude of sound in the i direction is proportional to the time derivative of force oriented in the i direction [$\delta F(i)/\delta t$], and inversely proportional to cr.

Acoustic compactness assumption

To test this model's assumption that $ka<<1$, wing length, f, and body mass were obtained from the literature for a range of birds and insects (Greenewalt, 1962; Pennycuick, 1990).

Hovering hummingbird hum

We tested our model by comparing the wing hum of a hovering hummingbird with the predicted wing hum from a CFD model. Song et al. (2014) used a CFD model to estimate the non-dimensional wing forces $F(i,t)$ of a hovering male Ruby-throated hummingbird (*Archilochus colubris*; assuming body mass: 2.7 g, wingbeat frequency: 57 Hz) in the three cardinal directions around the bird ($i=x, y, z$). We re-scaled their data (in amplitude) to produce weight support in z for a female Costa's hummingbird (*Calypte costae*: body mass: 3.2 g, wingbeat frequency: 37 Hz). We then inserted the resulting estimate of $F(i,t)$ from Song et al.'s (2014) CFD model into Eqn 2 to generate a predicted nearfield $P(i,t)$ for a hovering female Costa's hummingbird.

Empirical data

A female Costa's hummingbird, *Calypte costae* (Bourcier 1839), was recorded as she hovered, stationary, at a feeder inside a cage. The bird was released after recording. Recordings were conducted under UCR IACUC protocol 20160039 and USFWS and CDFW collecting permits. These recordings were taken in the middle of a small room (approximately 5×5×3 m) in a building lacking HVAC equipment at the Boyd Deep Canyon Natural History Reserve (doi:10.21973/N3V66D). Recordings were made on a windless day, after switching off sound sources (such as computers), minimizing environmental background sounds. Thus, although this space was not anechoic, it provided low background sound levels (<20 dB re. 20 µPa), in which the bird's wing hum was the dominant sound within the room. The recordings were taken with two ½ inch free-field microphones (Brüel & Kjaer 4190; Nærum, Denmark) with a noise floor of 14.6 dB and sensitivity of 50 mV Pa^{-1}. The microphone below the bird was outfitted with a turbulence-reducing nose cone (Brüel & Kjaer UA 0386), which had no effect on its low frequency response, and no further acoustic shielding. Recordings from below the bird in which the bird's wake impinged directly on the microphone with audible microphone-

induced noise were not used. The recordings were made on a 24-bit recorder sampling at 96 kHz (Sound Devices 702; Reedsburg, WI, USA). The recorder's lowest frequency was 10 Hz, whereas the microphone had a flat frequency–response curve that extended below this value. The two microphones were placed in different configurations, 0.15 to 0.21 m from the bird (i.e. in the nearfield), to record from the three cardinal directions (during different bouts of hovering). The floor and walls were >1 m from the subject, such that reflected farfield sound traveled at least 2 m before returning to the microphone, and thus was ≥20 dB below directly transmitted sound (assuming it diminished as r^{-1}).

Sound pressure level (SPL) was calculated from power spectra of sounds in Raven 1.4 (Charif et al., 2008) with a FFT window of 65,536 samples. SPL was calculated relative to calibration recordings of known SPL produced with a B&K 4231 sound level calibrator (re. 20 µPa) (Clark et al., 2013).

Sound of hovering

During hovering, an animal produces sufficient aerodynamic force oriented on its *z*-axis to exactly offset its body weight (mass×gravitational acceleration, $\boldsymbol{mg}$, ∼10 m s^{-2}). Hence, at distance *r* below the hovering animal, there is an average increase in pressure $\bar{P}(z)$ above ambient P_0, where $[\bar{P}(z) - P_0]$ is proportional to body weight ($\boldsymbol{mg}$) and inversely proportional to distance (Eqn 3) or distance squared (Eqn 2). As microphones are high-pass instruments, if the animal hovers for a 'long' time (such as >1 s), a microphone with a minimum frequency of 10 Hz will quickly lose the initial transient change in mean pressure from P_0 to $\bar{P}(z)$ associated with the onset of hovering (Fig. 4A). That is, a microphone cannot measure $\bar{P}(z)$ directly. $\bar{P}(z) - P_0$ can instead be estimated from the time course of force production by the wings $P_{\mathrm{hov}}(z)$, by assuming that during hovering the fluctuations in $P_{\mathrm{hov}}(z)$ around $\bar{P}(z)$ are similar in magnitude to $\bar{P}(z) - P_0$.

The dominant harmonic (n) of the Gutin sound is either the fundamental wingbeat frequency (n=1f) or, in special cases such as species with an active upstroke (or dragonflies: see Discussion), twice the fundamental frequency (n=2f), such as the hummingbird data reported here (see Results). For the purposes of modeling, we assumed wing force is produced sinusoidally at n=1f with a minimum force of zero and a maximum of 2 $\boldsymbol{mg}$. In this case, as the animal is supporting body weight, $F(z,t)=\boldsymbol{mg}\sin(\omega t)$, the time derivative is $\partial F(z)/\partial t=\omega \boldsymbol{mg}\cos(\omega t)$, where ω is the angular frequency ($2\pi f$) of the wingbeat. Inserting these terms into Eqn 1, again assuming M and $\delta Q/\delta t$ are negligible, the Gutin sound model predicts the sound field $P_{\mathrm{hov}}(z,t)$ at distance z below the hovering animal:

$$P_{\mathrm{hov}}(z,t) = \frac{\boldsymbol{mg}\,\sin\,\omega t}{4\pi r^2} + \frac{f\boldsymbol{mg}\,\cos\,\omega t}{2cr}. \quad (4)$$

The left-hand term containing sin is the nearfield, and the right-hand term containing cos is the farfield. The nearfield–farfield transition (in which the two terms are equal in magnitude) occurs at $r=\lambda/2\pi n$, where n=1 for the fundamental frequency, n=2 for the 2nd harmonic, etc. We assessed the predictions made by this sinusoidal force model against published empirical data for mosquitoes (Arthur et al., 2014), birds and bats (Boonman et al., 2020, 2018; LePiane and Clark, 2020).

RESULTS

From eagles to mosquitoes, the Helmholtz number of birds and insects is invariant with body size (Fig. 2). Within the first six harmonics (i.e. n=1…6) of their wingbeat, birds and insects are acoustically compact; the Helmholtz number of the fundamental frequency (1f) varied between 0.02 and 0.07 among most animals sampled (Fig. 2B) (the greatest outliers are butterflies, with their low wingbeat frequencies, where $ka\approx0.01$). These data show that birds and insects have a maximum spatial extent that is much smaller than the wavelength of sound produced by their flapping wings. Because animals are compact sound sources, interference between the wings is low, while the 'reactive nearfield' (nearfield effects caused by high particle velocity magnitudes) will be substantial (Larsen and Wahlberg, 2017).

The functional form of the predicted $P(i,t)$ from Song et al.'s (2014) CFD model is a qualitative match to our measured $P(i,t)$ of a female Costa's hummingbird in all three dimensions (Fig. 3). The predicted nearfield wing sound derived from Song et al.'s (2014) model, scaled to a unit distance of r=1 m, is shown in Fig. 3A, with downstroke depicted with gray shading (note: recordings were taken at distances of 0.15–0.21 m; had we recorded at 1 m distance, farfield sound would have not been negligible). Three representative acoustic traces (from two different bouts) of the hovering Costa's hummingbird are shown in Fig. 3B. Recordings of hummingbird wing hum from the three cardinal directions are included in Audio 1–3. Wing sounds were at the highest amplitude in the 1st harmonic in the x direction, the 2nd harmonic was higher in the y direction, and in z, the amplitude of the first two harmonics was similar, 62.6 and 63.1 dB (Fig. 3C). Cumulatively the first six harmonics in the z direction sum to 70.5 dB (r=0.21 m); harmonics above the 6th were sufficiently low amplitude (in all three dimensions) that we ignored them. Two wingbeats (onset of downstroke aligned by eye) are shown in Fig. 3D, while Fig. 3E shows a comparison of model and data. Quantitatively, the amplitude of the sound recording in the i=x and z directions is 1.75 times (2 dB) the amplitude of predicted nearfield values from our model.

Sound of flying insects, birds and bats

Eqn 4 predicts the Gutin sound below the animal, from its body mass and wingbeat frequency. How far does this model predict wing sound will propagate? A mosquito flapping its wings at 1 kHz would be faintly audible at 20 dB (re. 20 µPa) against the background sound of a quiet room. Therefore, we defined the 20 dB distance as the distance r at which the farfield P_{hov} reaches 20 dB (Fig. 5A) (at $r<<\lambda/2\pi$, the nearfield term is negligible). Among the birds and insects sampled, the 20 dB distance varied primarily as a function of body weight, because weight determines the total aerodynamic force in z the animal needs to produce with its wings to remain aloft. Albatrosses or eagles have wingbeat frequencies as low as 2 Hz, so would have 20 dB distances of up to 1 km, while among the smaller animals capable of hovering, hummingbird wing hum (f of 25–100 Hz) is predicted to reach 20 dB approximately 10 m from the animal. Bees (e.g. *Bombus* spp., f: 200 Hz) have wing sounds that reach 20 dB at distances of 1–4 m, while mosquito wing sounds (f: 400–1000 Hz) are predicted to reach 20 dB at roughly 0.1–0.3 m (Fig. 5).

The nearfield sound amplitude is proportional to $\boldsymbol{mg}$ irrespective of f, thus the curves of predicted sound levels for different animals in Fig. 5B are strictly in order of body mass. Farfield sound is proportional to $\boldsymbol{mfg}$ (Eqn 4); therefore, although body mass is a strong determinant of the functional form shown in Fig. 5C, the curves are not strictly in order of body mass. Species with f that is low for their body mass (e.g. butterfly, *Pieris napi*) have proportionally lower amplitude of farfield sound and, conversely, species with high f for their body size (e.g. mosquito, *Aedes aegypti*)

Journal of Experimental Biology (2020) 223, jeb214965. doi:10.1242/jeb.214965

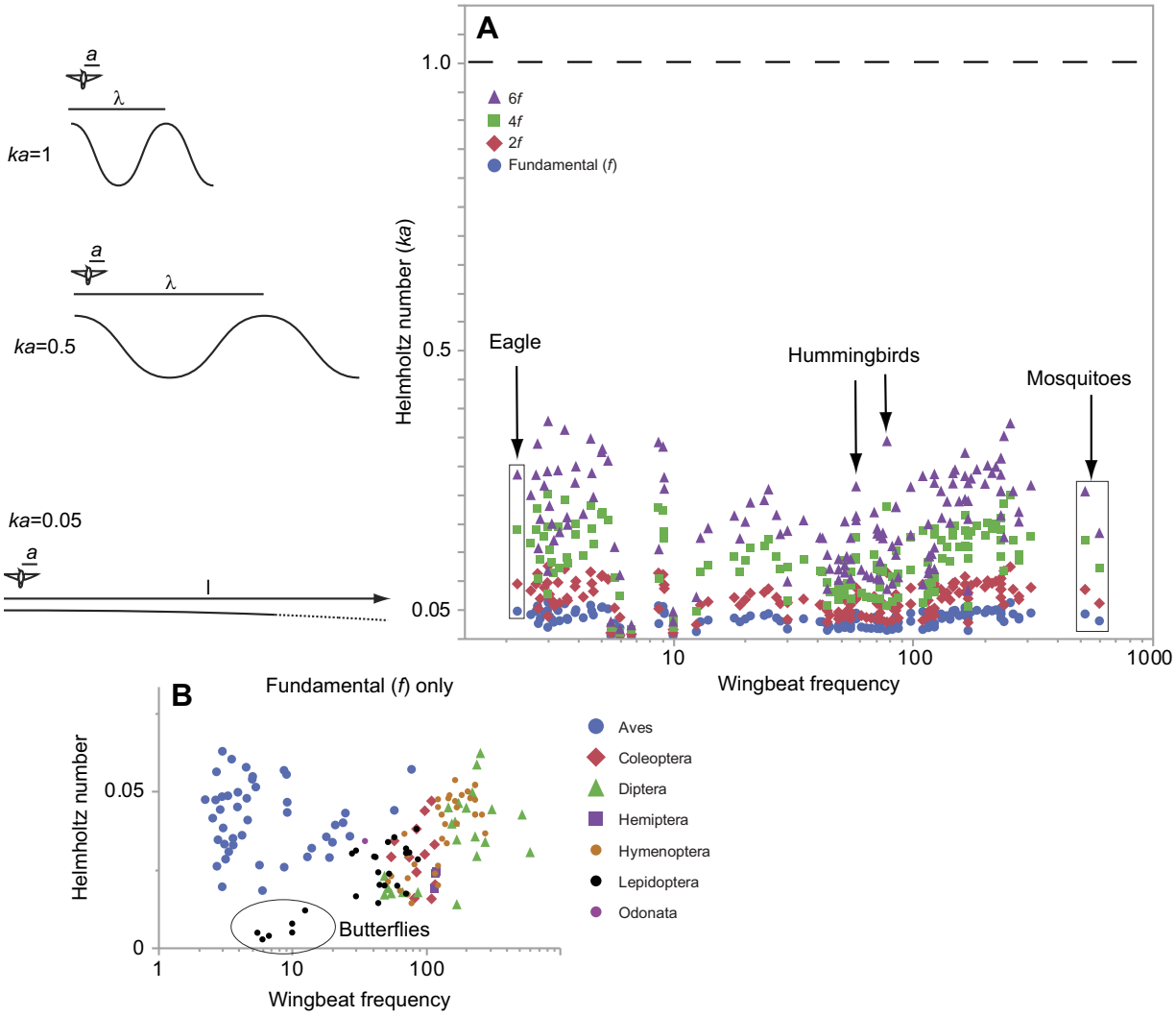

Fig. 2. From eagles to mosquitoes, the Helmholtz number of flying birds and insects is below 1. (A) The Helmholtz number, or *ka* product (Larsen and Wahlberg, 2017), is a dimensionless number describing the ratio of sound source size (*a*, wing length) relative to the wavelength of sound, λ (cartoon on left). *k* is wavenumber, $k=2\pi/\lambda$; $\lambda=c/nf$, c=340 m s^{-1} in air, *f* is wingbeat frequency, and *n* is the harmonic (n=1, 2, 4, 6 are shown). $ka \ll 1$ for birds and insects for $n \leq 6$; harmonics above the 6th are neglected as they appear to be a negligible component of wing motion (Fig. 3C). (B) Same data for n=1 only. The *ka* product of the fundamental of the wingbeat frequency for most birds and insects falls between 0.02 and 0.07. Therefore, flying birds and insects are acoustically compact: small relative to the wavelength of sound generated by their wings. Data are from Greenewalt (1962) and Pennycuick (1990).

have elevated farfield sound (Fig. 5C). This farfield dependence on *f* also means that harmonics above the fundamental contribute disproportionately to farfield sound (Fig. 6B).

The empirical measurements of wing SPL we found in the literature are presented in Fig. 6 and Table S1. Among these, wing sounds have been recorded on insects that are tethered or perched (e.g. honeybee waggle dance wing sound) and therefore do not support their weight while flapping. Arthur et al. (2014) recorded wing tone from a tethered mosquito at distances spanning the nearfield–farfield transition. Their data in the *z* direction are a good quantitative fit to our model (Fig. 6A), as are the shapes of their waveforms in *x* and *y* (fig. 5A of Arthur et al., 2014).

Boonman et al. (2018) recorded wing sound from underneath a barn owl taking off. Their sound amplitudes are substantially below the predicted values in *z* (Fig. 6C). LePiane and Clark (2020) recorded from underneath barn owls as they flew over a microphone, with values closer to those predicted by the hovering model, with an exponent of −1.1. Boonman et al. (2020) recorded wing sounds of four bird and three bat species in forward flight, from an oblique angle which changed with distance. Their data and our prediction for sound in *z* are shown in (Fig. 6D); their empirical exponent varied between −1.0 and −2.3 among the species measured.

DISCUSSION

We have developed a simple model for the sound field below an animal made by the fluctuating aerodynamic forces of flapping wings of a hovering animal. Nearfield recordings of the humming of hummingbirds and mosquitoes are consistent with this relatively simple model, which ignored the relative motion of the wings (we set M=0), assumed force was produced sinusoidal, ignored contributions of thickness noise or unsteady induced flow (the $\delta Q/\delta t$ term in Eqn 1) (Figs 3 and 6), ignored retarded time (which is the propagation delay between source and receiver), and ignored the presence of more than one wing.

The most general prediction this model makes seems to answer the question posed in the Introduction: one source of wing

Journal of Experimental Biology (2020) 223, jeb214965. doi:10.1242/jeb.214965

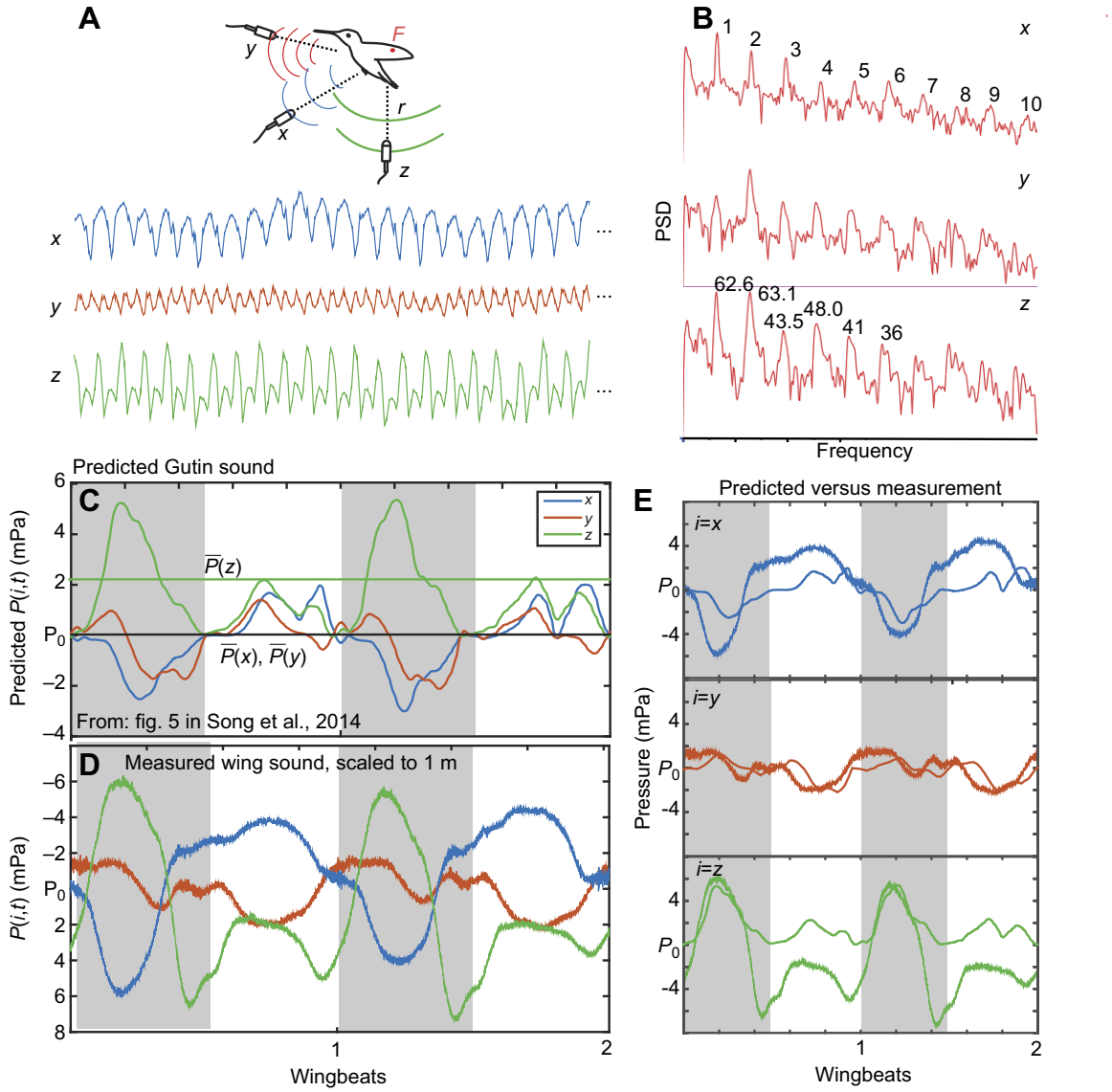

Fig. 3. Hummingbird wing hum and the Gutin sound model (nearfield). (A) A female Costa's hummingbird (*Calypte costae*) was recorded hovering at a feeder in a quiet room, with two B&K 4190 microphones placed in three locations (over multiple hovering trials) at a scalar distance between source and receiver r=0.15–0.21 m from the bird. The three representative sound traces of hovering shown were not recorded simultaneously. (B) Power spectral density (PSD) of wing sound in x, y and z, showing relative strength of first 10 harmonics. Source sound recordings are included in Audio 1–3. The 1st harmonic is highest in x; the 2nd harmonic is highest in y; and in z, the amplitude of the first six harmonics is indicated (re. 20 μPa): the 2nd harmonic is slightly higher (63.1 dB) than the 1st harmonic (62.6 dB). (C) Predicted Gutin sound (nearfield), derived from fig. 5A,B in Song et al. (2014), who used wing kinematics of a male Ruby-throated hummingbird (*Archilochus colubris*, body mass: 2.7 g, wingbeat frequency: 57 Hz) and a computational fluid dynamics (CFD) model to calculate normalized force components for a single flapping hummingbird wing, in the i=x, y and z directions. Their data were re-scaled in amplitude to produce weight support in z (i.e. mean z value is equal to $m\boldsymbol{g}$, where m is mass and $\boldsymbol{g}$ is gravitational acceleration) for female Costa's hummingbird (body mass: 3.2 g, wingbeat frequency: 37 Hz). After re-scaling in amplitude, the $F(z,t)$ from Song et al. (2014) was inserted into Eqn 2 to generate nearfield $P(i,t)$ shown. Note that mean modeled pressure produced in z, $\bar{P}_{hov}(z)$, is offset from ambient pressure (P_0) by approximately 2 mPa, a value sufficient to support body weight (see Fig. 4). (D) Microphone recordings for two wingbeats (note: not recorded simultaneously), re-scaled to a standard distance of r=1 m. (E) Model and empirical data for x, y and z. The bird is hovering, therefore the modeled pressure in x and y fluctuates around ambient pressure (P_0), while mean modeled pressure produced in z, $\bar{P}_{hov}(z)$, is offset from P_0 by a value sufficient to support body weight. As microphones measure relative pressure, measured $P_{hov}(z)$ fluctuates around 0.

tone is the time course of aerodynamic force production of the wings. As the wings reciprocate back and forth and are rotated at the end of the stroke, they produce an aerodynamic force vector that fluctuates in magnitude and direction. The aerodynamic pressure response therefore also fluctuates in each of the cardinal directions around the animal (x, y, z) in equal and opposite reaction to the wing aerodynamic forces. Aerodynamic effects that predominate on insect wings, such as the lift produced by wing rotation and vortex shedding, are intrinsically included in this model, as these mechanisms produce aerodynamic force and are not intrinsically different from other sources of lift and drag (Walker, 2002). For instance, periodic vortex shedding produces tonal sound, but not as a separate acoustic mechanism, because the way vortex shedding produces sound is by producing periodic cycles of lift and drag on the solid object (Blake, 2017a; Blake, 2017b, chapter 4). This mechanism provides a general explanation for why the flight tone in certain directions is, in many species, loudest (dominant) at the fundamental frequency of the wingbeat, while in other directions

Journal of Experimental Biology (2020) 223, jeb214965. doi:10.1242/jeb.214965

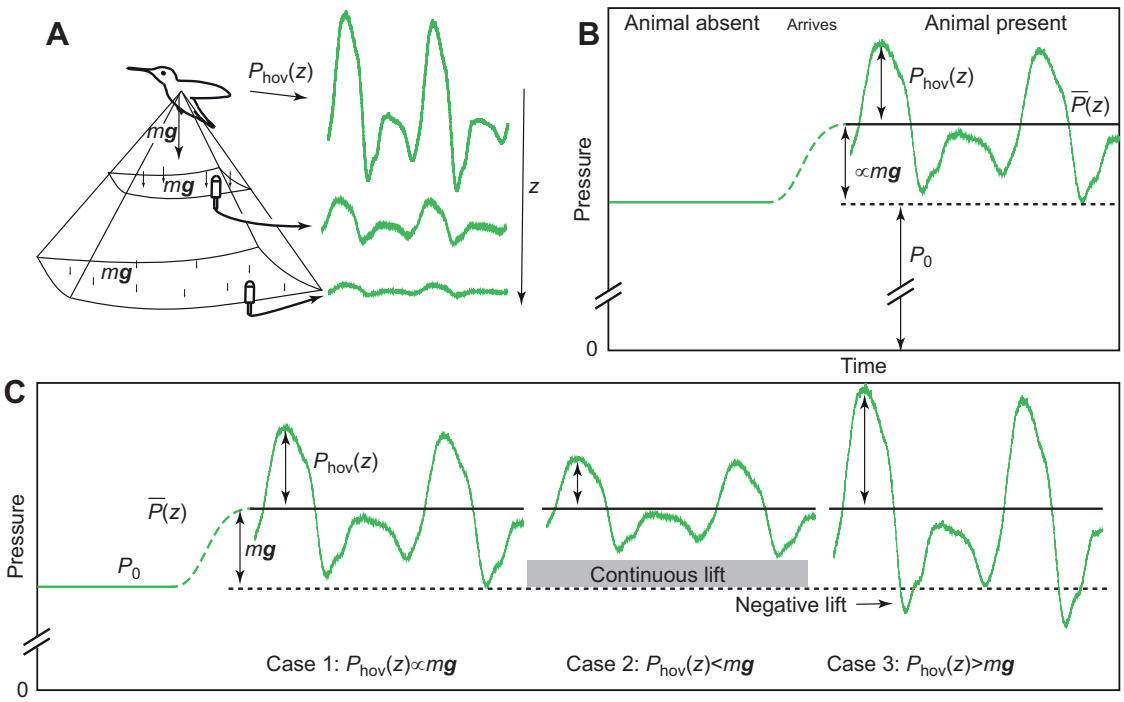

Fig. 4. The Gutin sound model, generalized for hovering. (A) A hovering animal supports its body weight, ***mg***. The aerodynamic force it exerts produces below it an average increase in pressure $\bar{P}_{hov}(z)$. This average increase in pressure, integrated across a suitable surface area, equals body weight. At increasing distances z below the animal, the suitable surface area increases, and local pressure decays as distance squared (z^{-2}) in the nearfield (Eqn 2), or z^{-1} in the farfield (Eqn 3). (B) Microphones are high-pass instruments and do not measure absolute pressure, such as atmospheric pressure (P_0) or $\bar{P}_{hov}$. Instead they measure relative pressure (P_{hov}) as it fluctuates around $\bar{P}_{hov}$. They also may measure the initial transient when the animal arrived or began to hover (green dashed line). (C) Assuming that body weight [$\bar{P}_{hov}(z) - P_0$] is proportional to $P_{hov}(z)$ provides a prediction of the acoustic amplitude of a hovering animal (case 1). Although case 1 is likely for hovering (see Discussion), it may not generalize to other modes of flight. In case 2, if force fluctuations do not descend as low as P_0 (i.e. some portion of lift is produced continuously), P_{hov} underestimates $\bar{P}(z)$, as is likely the case in forward flight, while in case 3, if a substantial amount of negative lift is produced (such as during the upstroke), P_{hov} overestimates $\bar{P}(z)$.

the flight tone is dominant at the 2nd harmonic of the fundamental frequency of the wingbeat, as previously noted in flies (Sueur et al., 2005), mosquitoes (Arthur et al., 2014), other insects (Sotavalta, 1952), and shown here for hummingbirds (Fig. 3). Which anatomical directions are fundamental-dominant versus 2nd harmonic-dominant depends on the time course of force production of the species in question.

An interesting theoretical case are four-winged insects such as dragonflies, in which ipsilateral (fore and hind) wings reciprocate with some independence, and flap at the wingbeat frequency but out of phase with each other. Independently reciprocating wings are similar to propellers that have multiple independent blades. The Gutin sound produced by a propeller is a collective product of all of the blades; hence, the frequency produced is the blade passage frequency, which is the rotation rate multiplied by the number of blades (Blake, 2017a; Gutin, 1948). In a dragonfly, assuming fore and hind wings produce similar amplitudes of lift, their wing tone is predicted to be at the even harmonics (2, 4, 6, etc.) of the wingbeat frequency, because their 'wing passage frequency' is double their wingbeat frequency.

Arthur et al. (2014) present detailed data on the wing sounds of tethered mosquitoes to which our model is a good fit (Fig. 6A). Many of the precise empirical details they report for mosquito wing tone are likely to be general to animal wing tones. They report that the phase relationships between the harmonics of wing sound are precise and fairly invariant (their Fig. 5). The flight stroke of flying animals has precise kinematics (such as timing of wing rotation) tuned to maximize useful aerodynamic forces (usually lift) and minimize not-useful forces (usually drag) produced by the wings. The waveforms of most hovering animals seem likely to resemble those shown in Fig. 3 (except for the dragonfly case described above). Deviating substantially from these phase relationships would produce an animal with mistimed wing kinematics that would tend to fail to produce sufficient aerodynamic force to remain aloft, or would produce high drag. This is not to say the phase relationships would be completely invariant; flying animals maneuver (turn, accelerate) by producing unbalanced forces with their contralateral (left, right) wings. This is achieved by subtly modifying the kinematics (varying amplitude and timing) of one wing relative to the other (Altshuler et al., 2012), which has the effect of causing phase between the harmonics to vary subtly. Moreover, as tethered animals do not support their body weight and may attempt to maneuver in ways that likely vary in time and between animals, completely invariant phase relationships in recordings of a tethered animal are not expected.

Arthur et al. (2014) suggested that their mosquito wing tone attenuated slightly faster than the square of distance (exponent of −2.3 to −2.5) over the distances at which they measured sound (their data are re-plotted in Fig. 6A). Our model suggests the rate of attenuation of the nearfield Gutin sound in the z direction is with the square of distance ($\propto r^{-2}$), and in the farfield (r>0.07 m), attenuates as r^{-1}. The slight discrepancy in exponent between Arthur et al.'s (2014) data and our model could be caused by an additional source of pressure close to the animal that decays with a higher exponent. Alternately, it could be caused by slight measurement error. Overall, their data are a good fit to the predicted exponent of −2 (Fig. 6A).

Journal of Experimental Biology (2020) 223, jeb214965. doi:10.1242/jeb.214965

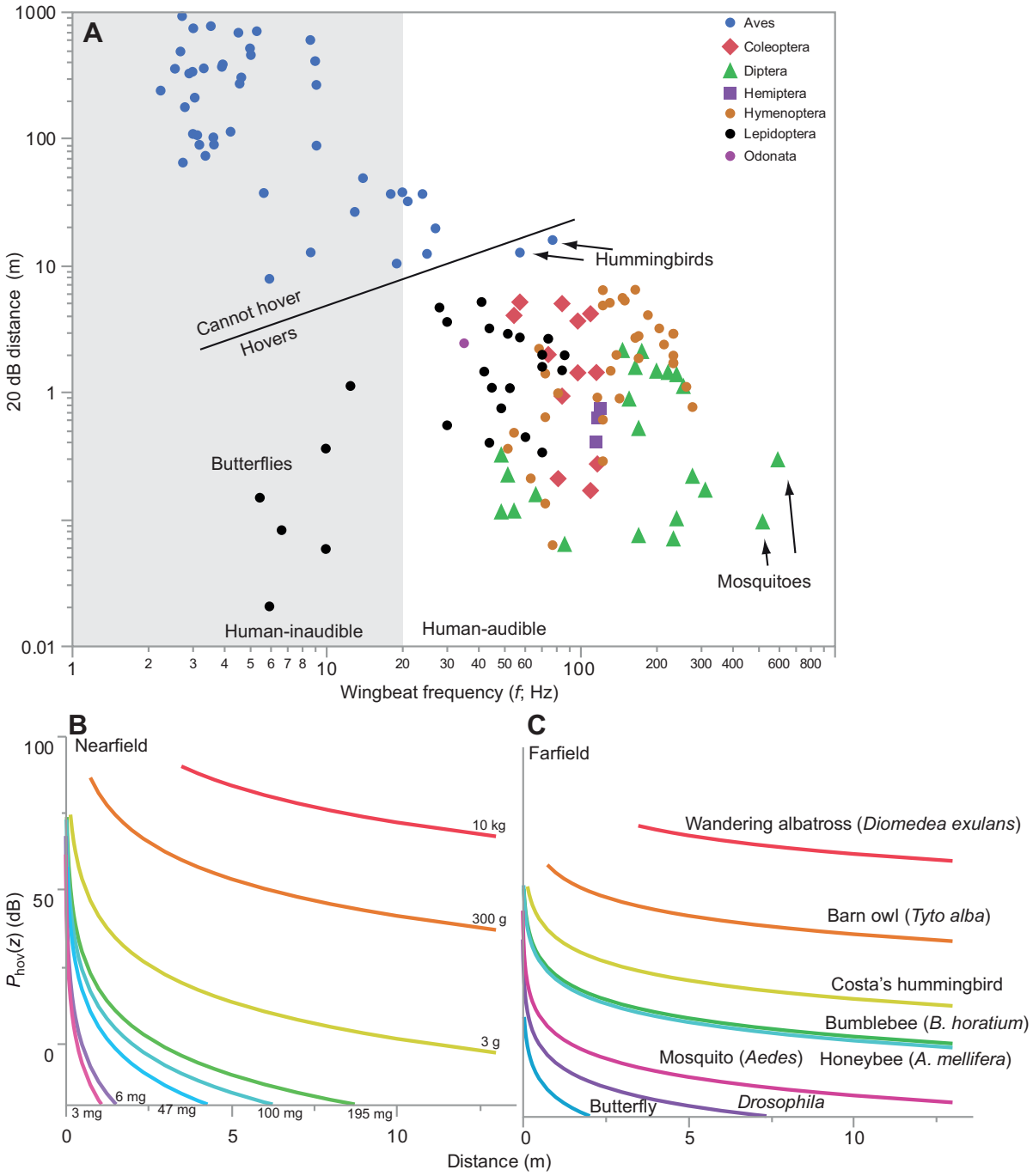

Fig. 5. Predicted Gutin sound below (*i*=*z*) a hovering animal for *n*=1*f*, assuming force is produced sinusoidally (Eqn 4). (A) Distance at which the farfield Gutin sound levels fall to 20 dB for animals varying in mass and wingbeat frequency. Data are from Greenewalt (1962) and Pennycuick (1990). (B) Predicted nearfield and (C) farfield sound pressure level (SPL) as a function of distance for a range of body masses. Nearfield and farfield sound have equal magnitude at $\lambda/2\pi$ (see Fig. 6). Butterfly is modeled on *Pieris napi*.

Our model provides a fit to Arthur et al.'s (2014) data that is similar to the FW–H model of Seo et al. (2019) of Arthur et al.'s (2014) data (dashed lines in Fig. 6A). The mismatch between the model and empirical data for birds and bats (Fig. 6C,D) has multiple simple explanations. Boonman et al.'s (2018, 2020) data are lower than the predicted values, but they recorded birds and bats with microphones with frequency–response curves that were flat down to 50 Hz (Boonman et al., 2018) and 40 Hz (Boonman et al., 2020), respectively, above the wingbeat frequencies of the species they measured. Moreover, Boonman et al. (2020) recorded from an oblique angle, while Fig. 6D shows the model's prediction in z. Although the Gutin sound in x and y of mosquitoes or hummingbirds is of the same order of magnitude as the Gutin sound in z (Fig. 3; Arthur et al., 2014), this did not seem to be the case for barn owls in forward flight (LePiane and Clark, 2020). If the Gutin sound of birds or bats is more directional than that of insects, it could provide another simple reason why Boonman et al.'s (2020) measured sound levels are well below the model predicted values in z. The model is for hovering, but both LePiane and Clark (2020) and Boonman et al. (2020) measured animals as

Journal of Experimental Biology (2020) 223, jeb214965. doi:10.1242/jeb.214965

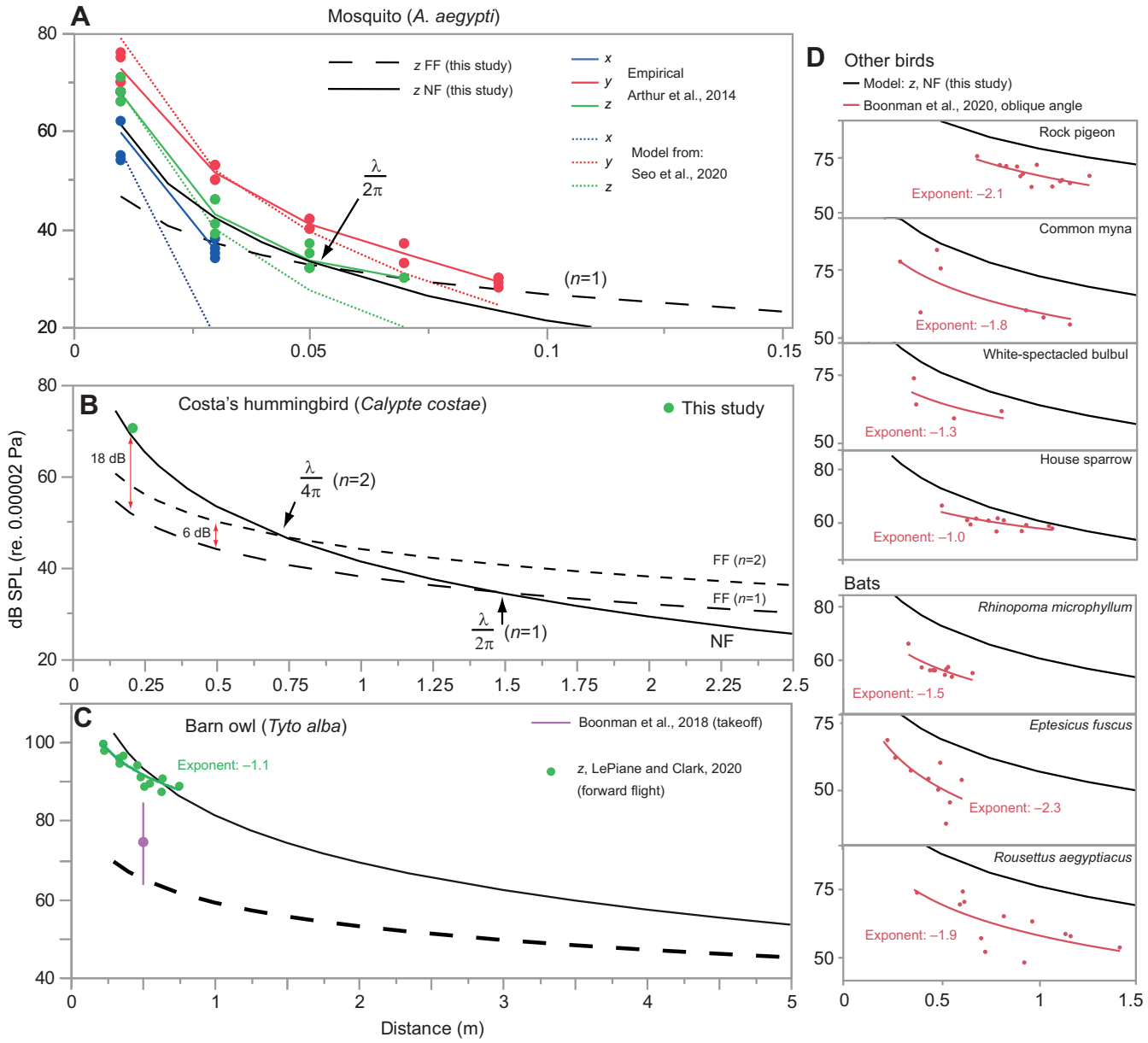

Fig. 6. Model predictions and empirical data for nearfield (solid line) and farfield (dashed line) sound of hovering. The nearfield–farfield transition is at $\lambda/(2\pi n)$. (A) Empirical data for *Aedes aegypti* from fig. 4A,C of Arthur et al. (2014) (data for males and females combined). dB sound velocity pressure levels of fundamental frequency (re. 5×10^{-8} m s^{-1}) of mosquito wing sounds in *x*, *y* and *z* (blue, red and green, respectively), against the predicted Gutin sound of hovering (converted to SPL, assuming impedance z_0=413 rayl and a body mass of 3 ***mg***). Colored dotted lines: Seo et al.'s (2019) FW–H model of Arthur et al.'s (2014) data (males only). Seo et al.'s (2019) exponents are −3.8 (*x*), −2.8 (*y*) and −2.8 (*z*). FF, farfield; NF, nearfield. (B) This study (Fig. 3). FF shown for two idealized conditions: P_{hov} is produced sinusoidally at *n*=1 (lower dashed line), and the 2nd harmonic, *n*=2 (higher dashed line). FF (*n*=2) is 6 dB higher than FF (*n*=1) for all distances. At *r*=0.21 m (distance at which empirical measurements took place), FF (*n*=1) is 18.0 dB lower than the NF (solid line). (C) Barn owl wing sounds from Boonman et al. (2018) and LePiane and Clark (2020). Boonman et al. (2018) recorded owls taking off (purple dot: mean; bar: range). As their microphone was sensitive down to 50 Hz, above the wingbeat frequency (4 Hz) of this species, their recordings underestimated the NF SPL levels present. Green dots: two owls recorded in *z* by LePiane and Clark (2020) in flapping flight, with a mean (±s.d.) flight velocity of 2.5±0.4 m s^{-1}. The microphone used had a flat frequency response down to 10 Hz. Exponent: −1.1. (D) Recordings of four birds and three bats by Boonman et al. (2020), from an oblique angle. Empirical estimate of exponent from a log fit varied between −1.0 (house sparrow) to −2.3 (*Eptesicus* bat).

they flew past a single microphone. In both these studies, orientation co-varied with distance, which might explain why the exponent among the species shown in Fig. 6C,D varied from −1.0 to −2.2.

The model presented here is a minimum model: animals that produce fluctuating aerodynamic forces with their wings to remain aloft must produce the fluctuating pressure modeled here (subject to the assumption about lift shown in Fig. 4C). Flying animals may produce additional sounds, via a variety of mechanisms. For instance, our model seems to adequately describe the hum of hummingbirds, but it appears to not entirely explain another familiar insect wing sound: the buzzing flight sound of bees and large flies. To human ears, Gutin sound is like a hum, because wing motions can be adequately described by roughly the first six harmonics of motion (Fig. 3C; Bae and Moon, 2008). The buzzing characterizing the wing sound of bees and flies arises from the presence of much

higher harmonics (far above 6*f*). It is these higher harmonics that makes them sound buzzy, rather than a hum, to human ears. These higher harmonics are not predicted by our model, implying they are not Gutin sound. They may not be produced the wings: some bees engage in 'buzz pollination' in which they audibly make buzzing sounds that resemble their flight sound when their wings are folded (Burkart et al., 2011), suggesting that one major source of the buzzing of bees may be the thorax, rather than the wings.

Flight performance and sound

The sound modeled here is the equal, opposite aerodynamic reaction to the production of aerodynamic force, the aerodynamic equivalent to ground reaction forces produced during terrestrial locomotion. Use of force plates to measure the ground reaction forces of animal appendages is widespread in studies of terrestrial locomotion (Full and Tu, 1991). A similar technique for flyers would open up a range of new topics of study on birds, bats and, especially, insects. Lentink and colleagues have developed an 'aerodynamic force plate' (AFP) that measures the instantaneous total aerodynamic force when an animal flies above it (Chin and Lentink, 2019; Hightower et al., 2017; Lentink et al., 2015), by physically integrating pressure across the entire surface area above and below the animal. Limits to Lentink et al.'s (2015) method include the need to record on both sides of the animal within a confined space, the inability to resolve force produced by one wing relative to the other and, especially, the limits on the devices' ability to record the more subtle pressures produced by small animals (i.e. insects).

Whether the dynamic range of microphones might overcome this last limitation and permit direct estimates of flight force from wing sound in ways the AFP cannot is not immediately clear. Several assumptions of our model require further refinement. In the comparison between model and prediction in Fig. 3E, we disregarded the farfield sound, which was between −12 and −18 dB below nearfield sound at our measurement distance of r=0.21 m (Fig. 6B). The −18 dB estimate derived from assuming force is produced at n=1 (the fundamental frequency); the −12 dB estimate derives from assuming force is produced at n=2 (the 2nd harmonic). The data shown in Fig. 3C show the two harmonics are of similar magnitude in z, implying the actual amplitude of the farfield was between −12 and −18 dB. Accounting for it would require attention to phase differences between the nearfield and farfield. Inclusion of farfield sound would reduce the 2 dB discrepancy between model and measurement in the z direction. Other subtle discrepancies between model and measurement in Fig. 3E might arise from the basis for Song et al.'s (2014) computational fluid dynamics model of a hovering hummingbird, which was taken from a male Ruby-throated hummingbird, whereas we recorded wing sound from a female Costa's hummingbird. There are pervasive differences between the sexes in hummingbird flight: male hummingbirds have substantially higher wingbeat frequencies and shorter wings than females. That is, our assumption that our hummingbird was a scaled version of theirs might be problematic, as the role of wing rotation in force production is likely greater in animals with increased wingbeat frequencies. A better test of the model would be to simultaneously record kinematics for a CFD model, and record wing tone from the same animal.

The crucial assumption of our model is that the amplitude of $P(i, t)$ around $\bar{P}(z)$, which we called P_{hov}, is proportional to total force ($\boldsymbol{mg}$ in the case of hovering) and, hence, the magnitude of $P_{\mathrm{hov}} \propto \boldsymbol{mg} r^{-2}$ (nearfield) or $P_{\mathrm{hov}} \propto f \boldsymbol{mg} r^{-1}$ (farfield) (Fig. 4C). This approximation will underestimate $\boldsymbol{mg}$ if some portion of lift is produced continuously (rather than episodically) (Fig. 4C, case 2), or overestimate $\boldsymbol{mg}$ if the animal produces substantial negative lift at some point during the wingbeat (Fig. 4C, case 3). Although neither of these conditions seems likely to be general to hovering, case 2 is likely representative of sound on the animal's z-axis during forward flight, because the mean air flow across the wings is sufficient to produce some fraction of lift continuously.

The model presented here makes quantitative predictions for hovering (Fig. 6). While large birds such as albatrosses, eagles or barn owls do not hover, they do make Gutin sound in the modes of flight they do engage in, such as takeoff (Boonman et al., 2018) or forward flight (Boonman et al., 2020; LePiane and Clark, 2020). Eqn 1 can be applied to other scenarios. Consider an owl gliding at a constant velocity towards a mouse. When gliding, the owl does not hear its own Gutin sound, as its ears move in the same frame of reference as its wings. But the mouse is exposed to rising pressure caused by the owl's approach. When gliding at constant velocity, $F(i,t)$ is time invariant, $\delta F_i/\delta t$, $\delta Q/\delta t$ and $\delta M_i/\delta t$ are zero, and if it glides straight at the mouse, $M=M_r$, causing Eqn 1 to simplify to: $P(i,t)=F_i/[4\pi(1-M_r)^2 r^2]$. The increase in pressure at the mouse caused by the owl's approach is low in magnitude, as F_i in the direction parallel to the owl's forward trajectory corresponds to drag, which is lower in magnitude than lift. The sound is also very low frequency, as the time course of change of pressure is associated with only the decreasing r as the owl approaches.

Biological significance

Animals use sound in communication (wing tone may be selected for) and in predator–prey interactions (wing tone may be selected against). The sound modeled here is an intrinsic byproduct of producing oscillating aerodynamic force with flapping wings. Wing sounds have been evolutionarily co-opted for communication many times in birds (Clark, 2016, 2018), but it is usually not the Gutin sound itself that plays a communication role, presumably because it is low frequency. In insects, mosquitoes and midges communicate with Gutin sound (Cator et al., 2009; de Silva et al., 2015) in flight. As Seo et al. (2019) point out, harmonic frequencies propagate further than the fundamental frequency; thus, species selected to use Gutin sound for communication may be selected to adopt wing morphologies and kinematics that accentuate harmonic frequencies. In addition to mosquito wing sounds, wing-generated sounds that appear to be Gutin sound serve communication purposes in *Drosophila* courtship (Spieth, 1974) or the waggle dance of bees (Michelsen et al., 1986) (Table S1), and there may also be plants that respond to insect wing sounds (Veits et al., 2019).

Regarding hunting, insects such as mosquitoes that hunt on the wing will inevitably give off sounds to which their prey may be sensitive. For instance, caterpillars respond to tones between 50 and 900 Hz with anti-predator behaviors, the frequency range corresponding to the wingbeat frequency of insect predators and parasitoids of caterpillars, such as flies and wasps (Taylor and Yack, 2019, and references therein). Taylor and Yack (2019) present data suggesting monarch butterfly (*Danaus plexippus*) caterpillars are sensitive specifically to near-field sound. Our Eqn 4 provides an estimate of the nearfield sound a parasitoid or predator makes when approaching possible prey, based on the mass and wingbeat frequency of the predator. Detection of low-frequency nearfield sound (corresponding to insect wing hum) is widespread in invertebrates (Taylor and Yack, 2019). For instance, orb-spiders drop out of their web at the approach of a hermit hummingbird that is hunting them, reportedly in response to the wing hum (Stiles, 1995).

Owls and other nocturnal birds (Caprimulgiformes) seem to have evolved mechanisms to reduce aspects of their flight sounds (Boonman et al., 2018; Graham, 1934). As the Gutin sound modeled here is an inevitable result of the generation of oscillating aerodynamic force with flapping wings, the only way an animal may reduce its Gutin sound signature is by modifying the time course of the aerodynamic forces it produces with its wings, such as by gliding rather than flapping (as in the thought example presented above). As most birds have wingbeat frequencies below 20 Hz, the Gutin sounds they produce may often be at frequencies too low to be audible to prey. But this is not certain. For example, while most rodents have limited hearing below 1 kHz, desert rodents have independently evolved sensitive low-frequency hearing multiple times (Mason, 2016; Webster and Webster, 1980). Manipulating a kangaroo rat's (*Dipodomys*) hearing impairs its ability to evade an owl strike (Webster, 1962; Webster and Webster, 1971). Moreover, spiny mice (*Acomys cahirinus*) behaviorally react to the wing flaps of an owl taking off (Boonman et al., 2018; Ilany and Eilam, 2008). Whether these rodents detect owls by sensing the Gutin sound of their wings, rather than other higher-frequency sources of sound that an attacking owl makes, remains unclear.

Acknowledgements
We thank Jasmine Mitchell and Irini Saad for assistance with data collection, Al Muth for access to Boyd Deep Canyon, and Krista LePiane and Arjan Boonman for sharing data.

Competing interests
The authors declare no competing or financial interests.

Author contributions
Conceptualization: C.J.C.; Methodology: C.J.C.; Software: E.A.M.; Validation: E.A.M.; Formal analysis: C.J.C., E.A.M.; Investigation: C.J.C.; Resources: C.J.C.; Data curation: C.J.C., E.A.M.; Writing - original draft: C.J.C., E.A.M.; Writing - review & editing: C.J.C.; Visualization: E.A.M.; Supervision: C.J.C.; Project administration: C.J.C.

Funding
Initial complement funding was provided by University of California, Riverside.

Supplementary information
Supplementary information available online at
https://jeb.biologists.org/lookup/doi/10.1242/jeb.214965.supplemental

References
Altshuler, D. L., Quicazán-Rubio, E. M., Segre, P. S. and Middleton, K. M. (2012). Wingbeat kinematics and motor control of yaw turns in Anna's Hummingbirds (*Calypte anna*). *J. Exp. Biol.* **215**, 4070-4084. doi:10.1242/jeb.075044

Arthur, B. J., Emr, K. S., Wyttenbach, R. A. and Hoy, R. R. (2014). Mosquito (*Aedes aegypti*) flight tones: frequency, harmonicity, spherical spreading, and phase relationships. *J. Acoust. Soc. Am.* **135**, 933-941. doi:10.1121/1.4861233

Bae, Y. and Moon, Y. J. (2008). Aerodynamic sound generation of flapping wing. *J. Acoust. Soc. Am.* **124**, 72-81. doi:10.1121/1.2932340

Blake, W. K. (2017a). Chapter 6 - noise from rotating machinery. In *Mechanics of Flow-Induced Sound and Vibration*, Vol. 2, 2nd edn. (ed. W. K. Blake), pp. 505-658: Academic Press.

Blake, W. K. (2017b). *Mechanics of Flow-Induced Sound and Vibration*: Academic Press.

Bodony, D. J., Day, L., Friscia, A. R., Fusani, L., Karon, A., Swenson, G. W., , Jr, Wikelski, M. and Schlinger, B. A. (2016). Determination of the wingsnap sonation mechanism of the golden-collared manakin (*Manacus vitellinus*). *J. Exp. Biol.* **219**, 1524-1534. doi:10.1242/jeb.128231

Boonman, A., Zadicario, P., Mazon, Y., Rabi, C. and Eilam, D. (2018). The sounds of silence: Barn owl noise in landing and taking off. *Behav. Process.* **157**, 484-488. doi:10.1016/j.beproc.2018.06.011

Boonman, A., Yovel, Y. and Eitan, O. (2020). Wing-beat frequency and its acoustics in birds and bats. *Integr. Comp. Biol.*, icaa085. doi:10.1093/icb/icaa085

Burkart, A., Lunau, K. and Schlindwein, C. (2011). Comparative bioacoustical studies on flight and buzzing of neotropical bees. *J. Pollination Ecol.* **6**, 118-124. doi:10.26786/1920-7603(2011)17

Cator, L. J., Arthur, B. J., Harrington, L. C. and Hoy, R. R. (2009). Harmonic convergence in the love songs of the dengue vector mosquito. *Science* **323**, 1077-1079. doi:10.1126/science.1166541

Charif, R. A., Waack, A. M. and Strickman, L. M. (2008). *Raven Pro 1.3 User's Manual*. Ithaca, NY: Cornell Laboratory of Ornithology.

Chin, D. D. and Lentink, D. (2019). Birds repurpose the role of drag and lift to take off and land. *Nat. Commun.* **10**, 5354. doi:10.1038/s41467-019-13347-3

Clark, C. J. (2016). Locomotion-induced sounds and sonations: mechanisms, communication function, and relationship with behavior. In *Vertebrate Sound Production and Acoustic Communication*, Vol. 53 (ed. R. A. Suthers and T. Fitch), pp. 83-117. New York: Springer.

Clark, C. J. (2018). Signal or cue? Locomotion-induced sounds and the evolution of communication. *Anim. Behav.* **143**, 83-91. doi:10.1016/j.anbehav.2018.07.009

Clark, C. J. and Mistick, E. A. (2018). Kinematic control of male Allen's Hummingbird wing trill over a range of flight speeds. *J. Exp. Biol.* **221**, jeb173625. doi:10.1242/jeb.173625

Clark, C. J., Elias, D. O. and Prum, R. O. (2013). Hummingbird feather sounds are produced by aeroelastic flutter, not vortex-induced vibration. *J. Exp. Biol.* **216**, 3395-3403. doi:10.1242/jeb.080317

de Silva, P., Nutter, B. and Bernal, X. E. (2015). Use of acoustic signals in mating in an eavesdropping frog-biting midge. *Anim. Behav.* **103**, 45-51. doi:10.1016/j.anbehav.2015.02.002

Dudley, R. (2000). *The Biomechanics of Insect Flight: Form, Function, Evolution*. Princeton, NJ: Princeton University Press.

Ffowcs Williams, J. and Hawkings, D. L. (1969). Sound generation by turbulence and surfaces in arbitrary motion. *Philos. Trans. R. Soc. Lond. A* **264**, 321-342. doi:10.1098/rsta.1969.0031

Full, R. J. and Tu, M. S. (1991). Mechanics of a rapid running insect: two-, four- and six-legged locomotion. *J. Exp. Biol.* **156**, 215-231.

Glegg, S. and Devenport, W. (2017). Chapter 16: Open rotor noise. In *Aeroacoustics of Low Mach Number Flows* (ed. S. Glegg and W. Devenport), pp. xi-xiii: Academic Press.

Graham, R. R. (1934). The silent flight of owls. *J. R. Aeronaut. Soc.* **38**, 837-843. doi:10.1017/S0368393100109915

Greenewalt, C. H. (1962). Dimensional relationships for flying animals. In *Smithsonian Miscellaneous Collections*, Vol. 144, pp. 1-46. Smithsonian Institution.

Gutin, L. (1948). *On the Sound Field of a Rotating Propeller*, Vol. TM-1195. Washington DC: NASA.

Hightower, B. J., Ingersoll, R., Chin, D. D., Lawhon, C., Haselsteiner, A. F. and Lentink, D. (2017). Design and analysis of aerodynamic force platforms for free flight studies. *Bioinspir. Biomim.* **12**, 064001. doi:10.1088/1748-3190/aa7eb2

Howe, M. S. (2008). *Acoustics of Fluid-Structure Interactions*. Cambridge: Cambridge University Press.

Ilany, A. and Eilam, D. (2008). Wait before running for your life: defensive tactics of spiny mice (*Acomys cahirinus*) in evading barn owl (*Tyto alba*) attack. *Behav. Ecol. Sociobiol.* **62**, 923-933. doi:10.1007/s00265-007-0516-x

Inada, Y., Aono, H., Liu, H. and Aoyama, T. (2009). Numerical analysis of sound generation of insect flapping wings. *Theor. Appl. Mech. Jpn.* **57**, 437-447.

Larsen, O. N. and Wahlberg, M. (2017). Sound and sound sources. In *Comparative Bioacoustics: An Overview* (ed. C. Brown and T. Riede), pp. 3-61. Bentham Science Publishers.

Lentink, D., Haselsteiner, A. F. and Ingersoll, R. (2015). *In vivo* recording of aerodynamic force with an aerodynamic force platform: from drones to birds. *J. R. Soc. Interface* **12**, 20141283. doi:10.1098/rsif.2014.1283

LePiane, K. and Clark, C. J. (2020). Evidence that the dorsal velvet of Barn Owl wing feathers decreases rubbing sounds during flapping flight. *Integr. Comp. Biol.*, icaa045. doi:10.1093/icb/icaa045

Lighthill, M. J. (1962). The Bakerian lecture, 1961 Sound generated aerodynamically. *Proc. R. Soc. A* **267**, 147-182. doi:10.1098/rspa.1962.0090

Lowson, M. V. (1965). The sound field for singularities in motion. *Proc. R. Soc. Math. Phys. Eng. Sci. A* **286**, 559-572. doi:10.1098/rspa.1965.0164

Magliozzi, B., Hanson, D. B. and Amiet, R. K. (1981). Propeller and propfan noise. In *Aeroacoustics of Flight Vehicles: Theory and Practice*, Vol. 1 (ed. H. H. Hubbard), pp. 1-64. Hampton, Virginia: NASA.

Mason, M. J. (2016). Structure and function of the mammalian middle ear. I: Large middle ears in small desert mammals. *J. Anat.* **228**, 284-299. doi:10.1111/joa.12313

Michelsen, A., Kirchner, W. H. and Lindauer, M. (1986). Sound and vibrational signals in the dance language of the honeybee, Apis mellifera. *Behav. Ecol. Sociobiol.* **18**, 207-212. doi:10.1007/BF00290824

Myhrvold, N. P. and Currie, P. J. (1997). Supersonic sauropods? *Tail Dyn. Diplodocids Paleobiol.* **23**, 393-409. doi:10.1017/S0094837300019801

Nedunchezian, K., Kang, C.-K. and Aono, H. (2019). Effects of flapping wing kinematics on the aeroacoustics of hovering flight. *J. Sound Vib.* **442**, 366-383. doi:10.1016/j.jsv.2018.11.014

Pennycuick, C. J. (1990). Predicting wingbeat frequency and wavelength of birds. *J. Exp. Biol.* **150**, 171-185.

Sane, S. P. and Dickinson, M. H. (2001). The control of flight force by a flapping wing: lift and drag production. *J. Exp. Biol.* **204**, 2607-2626.

Sarradj, E., Fritzsche, C. and Geyer, T. (2011). Silent owl flight: bird flyover noise measurements. *AIAA J.* **49**, 769-779. doi:10.2514/1.J050703
Schmitz, F. H. (1981). Rotor noise. In *Aeroacoustics of Flight Vehicles: Theory and Practice* (ed. H. H. Hubbard), pp. 65-149. Hampton, Virginia: NASA.
Seo, J.-H., Hedrick, T. L. and Mittal, R. (2019). Mechanism and scaling of wing tone generation in mosquitoes. *Bioinspir. Biomim.* **15**, 016008. doi:10.1088/1748-3190/ab54fc
Song, J., Luo, H. and Hedrick, T. L. (2014). Three-dimensional flow and lift characteristics of a hovering ruby-throated hummingbird. *J. R. Soc. Interface* **11**, 20140541. doi:10.1098/rsif.2014.0541
Sotavalta, O. (1952). Flight-tone and wing-stroke frequency of insects and the dynamics of insect flight. *Nature* **170**, 1057-1058. doi:10.1038/1701057a0
Spieth, H. T. (1974). Courtship behavior in *Drosophila*. *Annu. Rev. Entomol.* **19**, 385-405. doi:10.1146/annurev.en.19.010174.002125
Stiles, F. G. (1995). Behavioral, ecological and morphological correlates of foraging for arthropods by the hummingbirds of a tropical wet forest. *Condor* **97**, 853-878. doi:10.2307/1369527
Sueur, J., Tuck, E. J. and Robert, D. (2005). Sound radiation around a flying fly. *J. Acoust. Soc. Am.* **118**, 530-538. doi:10.1121/1.1932227
Taylor, C. J. and Yack, J. E. (2019). Hearing in caterpillars of the monarch butterfly (*Danaus plexippus*). *J. Exp. Biol.* **222**, jeb211862. doi:10.1242/jeb.211862
Tucker, V. A. (1998). Gliding flight: speed and acceleration of ideal falcons during diving and pull out. *J. Exp. Biol.* **201**, 403-414.
Veits, M., Khait, I., Obolski, U., Zinger, E., Boonman, A., Goldshtein, A., Saban, K., Seltzer, R., Ben-Dor, U., Estlein, P. et al. (2019). Flowers respond to pollinator sound within minutes by increasing nectar sugar concentration. *Ecol. Lett.* **22**, 1483-1492. doi:10.1111/ele.13331
Walker, J. A. (2002). Rotational lift: something different or more of the same? *J. Exp. Biol.* **205**, 3783-3792.
Webb, J. C., Sharp, J. L., Chambers, D. L. Benner, J. C. (1976). Acoustical properties of the flight activities of the Caribbean fruit fly. *J. Exp. Biol.* **64**, 761-772.
Webster, D. B. (1962). A function of the enlarged middle-ear cavities of the kangaroo rat, *Dipodomys*. *Physiol. Zool.* **35**, 248-255. doi:10.1086/physzool.35.3.30152809
Webster, D. B. and Webster, M. (1971). Adaptive value of hearing and vision in kangaroo rat predator avoidance. *Brain Behav. Evol.* **4**, 310-322. doi:10.1159/000125441
Webster, D. B. and Webster, M. (1980). Morphological adaptations of the ear in the rodent family Heteromyidae. *Am. Zool.* **20**, 247-254. doi:10.1093/icb/20.1.247
Williams, C. M. and Galambos, R. (1950). Oscilloscopic and stroboscopic analysis of the flight sounds of *Drosophila*. *Biol. Bull.* **99**, 300-307. doi:10.2307/1538745